Submitted to the
XXII International Symposium on Lepton-Photon Interactions at High Energy
June 30-July 5, 2005, Uppsala, Sweden

Abstract: 277 **Session: QCD/HS**

Study of production properties of baryons decaying to strange particles in *ep* collisions at HERA

ZEUS Collaboration

Abstract

A study of states and enhancements reconstructed using the invariant-mass spectra associated with strange baryons has been performed in *ep* collisions with the ZEUS detector at HERA using an integrated luminosity of 121 pb^{-1}. The invariant-mass spectra were reconstructed in several kinematic regions with the main emphasis on the spectra which are sensitive to the production of pentaquarks. The candidate Θ^+ signal was found to be produced predominantly in the forward hemisphere in the laboratory frame. This is unlike the case for the $\Lambda(1520)$ or the Λ_c, and indicates that the Θ^+ may have an unusual production mechanism related to proton-remnant fragmentation.

1 Introduction

Recently, many experimental groups have made significant efforts to find new baryonic states which can be explained as consisting of five quarks. A number of experiments [1] including ZEUS [2] have reported narrow signals in the vicinity of 1530 MeV in the nK^+ and pK^0_S invariant mass spectra. The signals are consistent with the exotic pentaquark baryon state Θ^+ with quark content $uudd\bar{s}$ [3]. Several other experiments have searched for this state with negative results [4]. ZEUS have reported negative searches for other possible pentaquark states [5, 6].

Inclusive searches of pentaquarks and other exotic states in the HERA ep collider can benefit from several aspects as reported in a previous publication [7]. This paper describes an inclusive search for new states whose decay products include strange hadrons. The searches involving Ξ baryons have already been published [6]. The invariant-mass spectra were reconstructed in several kinematic regions with the main emphasis on spectra which are sensitive to the production of pentaquarks. The invariant masses of known states with similar decay channels as for pentaquarks were also studied in order to show the sensitivity to new resonances and to compare their respective production mechanisms.

ZEUS is a multipurpose detector described in detail elsewhere [8]. The main components used in the present study are the central tracking detector (CTD) [9] and the uranium-scintillator calorimeter (CAL) [10].

2 Data sample

The data sample for this analysis was taken during the 1996–2000 running period of HERA, and corresponds to an integrated luminosity of 121 pb^{-1}. The electron-beam energy was 27.5 GeV and the proton-beam energy was 820 GeV for the 96–97 running period and 920 GeV for the 98–00 running period.

In this analysis, the data sample was divided into two categories: photoproduction (PHP) and DIS. The latter sample was studied at low ($Q^2 > 1\,\text{GeV}^2$) and medium ($Q^2 > 20\,\text{GeV}^2$) values of the exchanged photon virtuality, Q^2.

The photoproduction sample, being the largest inclusive data sample taken by ZEUS, is required to have no scattered electron detected in the CAL. For this sample, a primary vertex position should be in the range $| Z_{\text{vertex}} | \leq 50\,\text{cm}$. To obtain as large as possible statistics, this data sample has no specific trigger requirements, but the events should pass through the standard ZEUS three-level trigger chain. This data sample is dominated by photoproduction events with low-E_T jets ($E_T > 6\,\text{GeV}$).

The hadronic final state in DIS events provides the most unbiased data sample for searches of new states. The kinematic variable Q^2 was reconstructed from the energy and angle of the scattered electron, which was identified from the pattern of energy deposits in the CAL [11]. This method is denoted by the subscript e. The following requirements were used to select neutral current DIS events:

- $E_{e'} \geq 8.5\,\mathrm{GeV}$, where $E_{e'}$ is the energy of the scattered electron;
- $\mid Z_{\mathrm{vertex}} \mid \leq 50$ cm, where Z_{vertex} is the vertex position determined from the tracks;
- $35 \leq \sum E_i(1-\cos\theta_i) \leq 60\,\mathrm{GeV}$, where E_i is the energy of the ith calorimeter cell, and θ_i is its polar angle with respect to the measured primary vertex position, and the sum runs over all cells;
- $Q_e^2 > 1\,\mathrm{GeV}^2$ or $Q_e^2 > 20\,\mathrm{GeV}^2$;
- $y_e \leq 0.95$ and $y_{\mathrm{JB}} \geq 0.01$, where the subscript JB denotes the Jacquet-Blondel method [12].

The present analysis was based on tracks measured in the CTD. All tracks were required to pass through at least three CTD superlayers. Only tracks with transverse momenta $p_T^{\mathrm{lab}} > 150\,\mathrm{MeV}$ were considered. The above cuts restricted this analysis to a region where the track acceptance and resolution of the CTD are high.

The energy-loss measurement in the CTD, dE/dx, was used for particle identification. Tracks with $f < dE/dx < F$, $dE/dx > 1.15$ mips and $p < 1.5\,\mathrm{GeV}$ were taken as (anti)proton candidates [2], where $f = 0.35/p^2 + 0.8$, $F = 1.0/p^2 + 1.2$ (for positive tracks), $f = 0.3/p^2 + 0.8$, $F = 0.75/p^2 + 1.2$ (for negative tracks) and p is the total track momentum in GeV. For the kaon candidates, $f = 0.1/p^2 + 0.8$, $F = 0.25/p^2 + 1.1$ and $dE/dx > 1.25$ mips are required. Pion candidates correspond to the tracks that do not pass the proton and kaon dE/dx requirements described above.

The K_S^0 mesons were identified by their charged decay mode, $K_S^0 \to \pi^+\pi^-$ using the pairs of tracks originating from secondary vertices. Both tracks were assigned the mass of the charged pion and the invariant mass, $M(\pi^+\pi^-)$, of each pair of tracks was calculated. The K_S^0 candidates were selected by imposing the following requirements [2]: $M(e^+e^-) \geq 50\,\mathrm{MeV}$, where the electron mass was assigned to each track, to eliminate tracks from photon conversions; $M(p\pi) \geq 1121\,\mathrm{MeV}$, where the proton mass was assigned to the track with higher momentum, to eliminate Λ and $\bar{\Lambda}$ contamination of the K_S^0 signal; $483 \leq M(\pi^+\pi^-) \leq 513\,\mathrm{MeV}$; $p_T(K_S^0) \geq 0.3\,\mathrm{GeV}$ and $|\eta(K_S^0)| \leq 1.5$. The $\pi^+\pi^-$ invariant-mass spectrum is very clean and almost background free [2]. About 4.4M K_S^0 candidates were reconstructed in both PHP and DIS samples.

The Λ baryons were identified by their charged decay mode, $\Lambda \to p\pi^-$, using pairs of tracks from secondary vertices. In order to further reduce background, the track with the higher momentum was required to have a dE/dx consistent with a proton and assigned a proton mass. After removing photon conversions as for the K_S^0 and pairs of tracks with $M(\pi^+\pi^-) \geq 483\,\mathrm{MeV}$, where the pion mass was assigned to each track, Λ candidates were reconstructed in the mass region $1111 \leq M(p\pi^-) \leq 1121\,\mathrm{MeV}$. The cuts were set to $p_T(\Lambda) \geq 0.3\,\mathrm{GeV}$ and $|\eta(\Lambda)| \leq 1.5$. The resulting invariant-mass spectra are shown in a previous publication [6]. About 840k $\Lambda(\bar{\Lambda})$ candidates were reconstructed in PHP and DIS.

3 Results

3.1 $K_S^0\, p$ mass spectra

Figure 1 shows the $K_S^0\, p\ (\bar{p})$ invariant-mass spectra for three data samples: 1) all data which passed the ZEUS trigger chain after removing DIS events. This data sample is dominated by PHP events as explained in Section 2; 2) DIS events with $Q^2 > 1\,\mathrm{GeV}^2$. This sample represents the largest DIS data sample taken; 3) DIS events at medium $Q^2 > 20\,\mathrm{GeV}^2$. The latter sample was used in the previous ZEUS publication [2].

The $K_S^0\, p\ (\bar{p})$ distribution has two peaks, at around $1522\,\mathrm{MeV}$ ($Q^2 > 20\,\mathrm{GeV}^2$) and at around $2286\,\mathrm{MeV}$ (PHP and DIS). The first peak is attributed to the Θ^+ (1520) state, which has been discussed in detail in the previous ZEUS publication [2]. The second peak, which corresponds to the established Λ_c, was fitted using a Gaussian with a second-order polynomial function for the background. Both peaks are best seen at $Q^2 > 20\,\mathrm{GeV}^2$. This is a region where the Λ_c peak has largest signal-over-background ratio (S/B=0.22). The signal-over-background ratio in PHP is rather small, since the average charged-track multiplicity in PHP is larger by 50% than in DIS at $Q^2 > 1\,\mathrm{GeV}^2$. Since the combinatorial background is larger for low Q^2 DIS and PHP, this may explain the non-observation of the Θ^+ for these two samples [2].

The Λ_c peak was further studied in the forward ($\eta > 0$) and in the rear ($\eta < 0$) pseudorapidity regions, shown in Fig. 2, and for protons and antiprotons, shown in Fig. 3. Due to low statistics, the peak position and the width were fixed from the fit to the overall mass spectra for $Q^2 > 1\,\mathrm{GeV}^2$ (shown in Fig. 1) in order to obtain stable fits. The numbers of the extracted Λ_c candidates are about the same for all four mass distributions. This indicates that the production of Λ_c is consistent with the fragmentation of $c(\bar{c})$ quarks produced by the boson-gluon-fusion mechanism, $\gamma^* g \rightarrow c\bar{c}$.

3.2 $K^- p$ mass spectra

Figure 4 shows the invariant mass of $K^- p$ (and $K^+ \bar{p}$) combinations for PHP and DIS ($Q^2 > 1\,\mathrm{GeV}^2$ and $Q^2 > 20\,\mathrm{GeV}^2$). The fits of the invariant-mass distributions shown in this figure lead to significant numbers of reconstructed $\Lambda(1520)$ baryons (13500 for PHP, 2600 for DIS). Unlike Λ_c, the signal-over-background ratio for $\Lambda(1520)$ is similar for PHP and DIS. This is possible if the production rate of the $\Lambda(1520)$ baryons is proportional to the energy available for the fragmentation process. This indicates that $\Lambda(1520)$ can be produced by pure fragmentation mechanism, without partons from the hard interaction.

The $\Lambda(1520)$ was also studied in the forward ($\eta > 0$) and in the rear $\eta < 0$ pseudorapidity regions, Fig. 5. There are similar numbers of $\Lambda(1520)$ candidates for these two pseudorapidity regions. Also the fits shown in Fig. 6 give similar numbers of $\Lambda(1520)$ baryons and antibaryons. Both observations strengthen the conclusion that the dominant production mechanism of $\Lambda(1520)$ is pure fragmentation.

3.3 Searches in $K^+ p$ and $\Lambda\pi$ mass spectra

The Θ^{++} state was searched in the $K^+ p$ ($K^- \bar{p}$) invariant-mass spectrum in PHP and DIS, Fig. 7. However, no signal was found in either distribution. This indicates that Θ^+ (1520) is not an isotensor.

If the peak in the $K^0_S\, p$ invariant mass spectrum near 1520 MeV corresponds to a new Σ state rather than to the strange pentaquark, the decay Θ^+ (1520) $\rightarrow \Lambda\pi^+$ should also be allowed. The $\Lambda\pi$ invariant mass is shown in Fig. 8. Peaks due to the known PDG states, $\Xi(1320)$ and $\Sigma(1385)$ baryons, are clearly seen. However, no statistically significant peak is seen near 1520 MeV.

For $Q^2 > 1\,\mathrm{GeV}^2$, an additional peak of low statistical significance ($4.4\,\sigma$) is observed near 1600 MeV, which is consistent with non-well established PDG $\Sigma(1580)$ or $\Sigma(1620)$ states [13].

3.4 Production properties of the Θ^+ candidate

If the observed $K^0_S p(\bar{p})$ peak near 1520 MeV corresponds to a new state, then the studies of this peak in different pseudorapidity regions, as well as for proton and antiproton samples, can help to qualify the production mechanism of this baryonic state. The 1520 MeV peak should be seen for both forward and rear pseudorapidity regions if the Θ^+ is produced by pure fragmentation without the diquark system from the proton remnant. In contrast, if the production mechanism of the Θ^+ (1520) state involves the fragmentation of the proton remnant, Θ^+ (1520) state should mainly be seen for $\eta > 0$ and at low transverse momenta. In addition, for the latter mechanism, the production rate of antibaryons should be suppressed compared to particles, and the high-Q^2 region is the most favorable for the Θ^+ (1520) production [7].

The results of the fits of the $K^0_S\, p$ invariant mass near 1520 MeV are shown in Fig. 9 for a region where the contribution from the proton remnant is expected to be more pronounced (the upper figure), and a region dominated by pure fragmentation (the bottom figure). The signal is found to occur predominantly in the first pseudorapidity region.

Figure 10 shows the signal separately for $K^0_S\, p$ and $K^0_S\, \bar{p}$ combinations, with the double-Gaussian fits [2]. The number of $K^0_S\, p$ candidates is distinctly larger than for $K^0_S\, \bar{p}$, however, no strong conclusion can be made since the background spectra for $K^0_S\, \bar{p}$ is too complicated near 1480 MeV region.

Finally, Figs. 11 and 12 show the invariant-mass spectra for $\eta > 0$ for protons and antiprotons. In Fig. 11, the fit was performed using one free parameter for the overall normalisation (other fitting parameters were fixed from the sum of the two distributions). The fit shown in Fig. 12 was performed using three free parameters: two for the number of combinations in the peaks and one for the background normalisation. The latter fit, which has the best χ^2/ndf, leads to $5.4\,\sigma$ statistical significance for the observed peak.

4 Conclusions

The invariant-mass spectra sensitive to possible baryonic states decaying to strange hadrons have been investigated. The candidate Θ^+ (1520) signal reported earlier [2] was found to be produced predominantly in the forward pseudorapidity region, unlike the well-established baryons, $\Lambda(1520)$ and Λ_c. This indicates that the Θ^+ may have an unusual production mechanism related to proton-remnant fragmentation. The production of Θ^- (1520) has lower rate relative to Θ^+ (1520), however, the statistical significance of this observation is low, and the background for antiproton spectra is too complicated to draw a strong conclusion.

As for the previous ZEUS studies [2], the candidate Θ^+ (1520) signal exists predominantly at medium Q^2 events. The studies of Λ_c indicate that combinatorial background for this Q^2 region is rather favorable for the reconstruction of a state whose production is not driven by pure fragmentation mechanism.

A significant number of $\Lambda(1520)$ baryons were reconstructed in the K^-p decay channel. There is a strong indication that the main production mechanism of this baryon is pure fragmentation. A search was performed for $\Theta^{++} \to K^+p$ signal, however, the results were negative.

The $K^0_S\,p$ peak near 1520 MeV could also be a new Σ state, which can decay to $\Lambda\pi$. To check this, $\Lambda\pi$ mass combinations were investigated for PHP and DIS. No significant peak near the Θ^+ (1520) mass region was found.

References

[1] LEPS Collaboration, T. Nakano, et al., Phys. Rev. Lett. **91**, 012002 (2003);
SAPHIR Collaboration, J. Barth, et al., Phys. Lett. **B572**, 127 (2003);
CLAS Collaboration, S. Stepanyan, et al., Phys. Rev. Lett. **91**, 252001 (2003);
CLAS Collaboration, V. Kubarovsky, et al., Phys. Rev. Lett. **92**, 032001 (2004);
DIANA Collaboration, V. V. Barmin, et al., Phys. Atom. Nucl. **66**, 1715 (2003);
SVD Collaboration, A. Aleev, et al., Preprint hep-ex/0401024, 2004. Submitted to Yad Fiz (2004);
HERMES Collaboration, A. Airapetian, et al., Phys. Lett. **B 585**, 213 (2004);
COSY-TOF Collaboration, M. Abdel-Bary, et al., Phys. Lett. **B 595**, 127 (2004);
A. E. Asratyan, A. G. Dolgolenko, M. A. Kubantsev, Phys. Atom. Nucl. **67**, 682 (2004).

[2] ZEUS Collaboration, S. Chekanov, et al., Phys. Lett. **B 591**, 7 (2004).

[3] D. Diakonov, V. Petrov, M. V. Polyakov, Z. Phys. **A 359**, 305 (1997).

[4] BES Collaboration, J. Z. Bai, et al., Phys. Rev. **D 70**, 012004 (2004);
HERA-B Collaboration, I. Abt, et al., Phys. Rev. Lett. **93**, 212003 (2004);
SPHINX Collaboration, Y. M. Antipov, et al., Eur. Phys. J. **A21**, 455 (2004);
ALEPH Collaboration, S. Schael, et al., Phys. Lett. **B 599**, 1 (2004);
D. O. Litvintsev, *Presented at 6th International Conference on Hyperons, Charm and Beauty Hadrons (BEACH 2004).* Chicago, Illinois, USA (2004). Also in preprint FERMILAB-CONF-04-205-E (hep-ex/0410024);
CDF Collaboration, I. V. Gorelov, Preprint hep-ex/0408025, 2004;
BABAR Collaboration, B. Aubert, et al., *Submitted to 32nd International Conference on High-Energy Physics (ICHEP 04).* Beijing, China (2004). Also in preprint hep-ex/0408064;
PHENIX Collaboration, C. Pinkenburg, J. Phys. **G30**, S1201 (2004).

[5] ZEUS Collaboration, S. Chekanov, et al., Eur. Phys. J. **C 38**, 29 (2004).

[6] ZEUS Collaboration, S. Chekanov, et al., Phys. Lett. **B 610**, 212 (2005).

[7] S. Chekanov, Preprint ANL-HEP-PR-05-06, hep-ph/0502098, 2005.

[8] U. Holm, et al. (eds.), *The ZEUS Detector.* Status Report (unpublished), DESY (1993), available on `http://www-zeus.desy.de/bluebook/bluebook.html`.

[9] N. Harnew, et al., Nucl. Instrum. Meth. **A 279**, 290 (1989);
ZEUS Collaboration, B. Foster, et al., Nucl. Instrum. Meth. **A 338**, 254 (1994).

[10] ZEUS Collaboration, M. Derrick, et al., Nucl. Instrum. Meth. **A 309**, 77 (1991);
ZEUS Collaboration, A. Andresen, et al., Nucl. Instrum. Meth. **A 309**, 101 (1991);
ZEUS Collaboration, A. Caldwell, et al., Nucl. Instrum. Meth. **A 321**, 356 (1992);
ZEUS Collaboration, A. Bernstein, et al., Nucl. Instrum. Meth. **A 336**, 23 (1993).

[11] H. Abramowicz, A. Caldwell, R. Sinkus, Nucl. Instrum. Meth. **A 365**, 508 (1995).

[12] F. Jacquet, A. Blondel, *Proceedings of the Study for an ep Facility for Europe*, U. Amaldi (ed.), p. 391. Hamburg, Germany (1979). Also in preprint DESY 79/48.

[13] Particle Data Group, S. Eidelman, et al., Phys. Lett. **B 592**, 4 (2004).

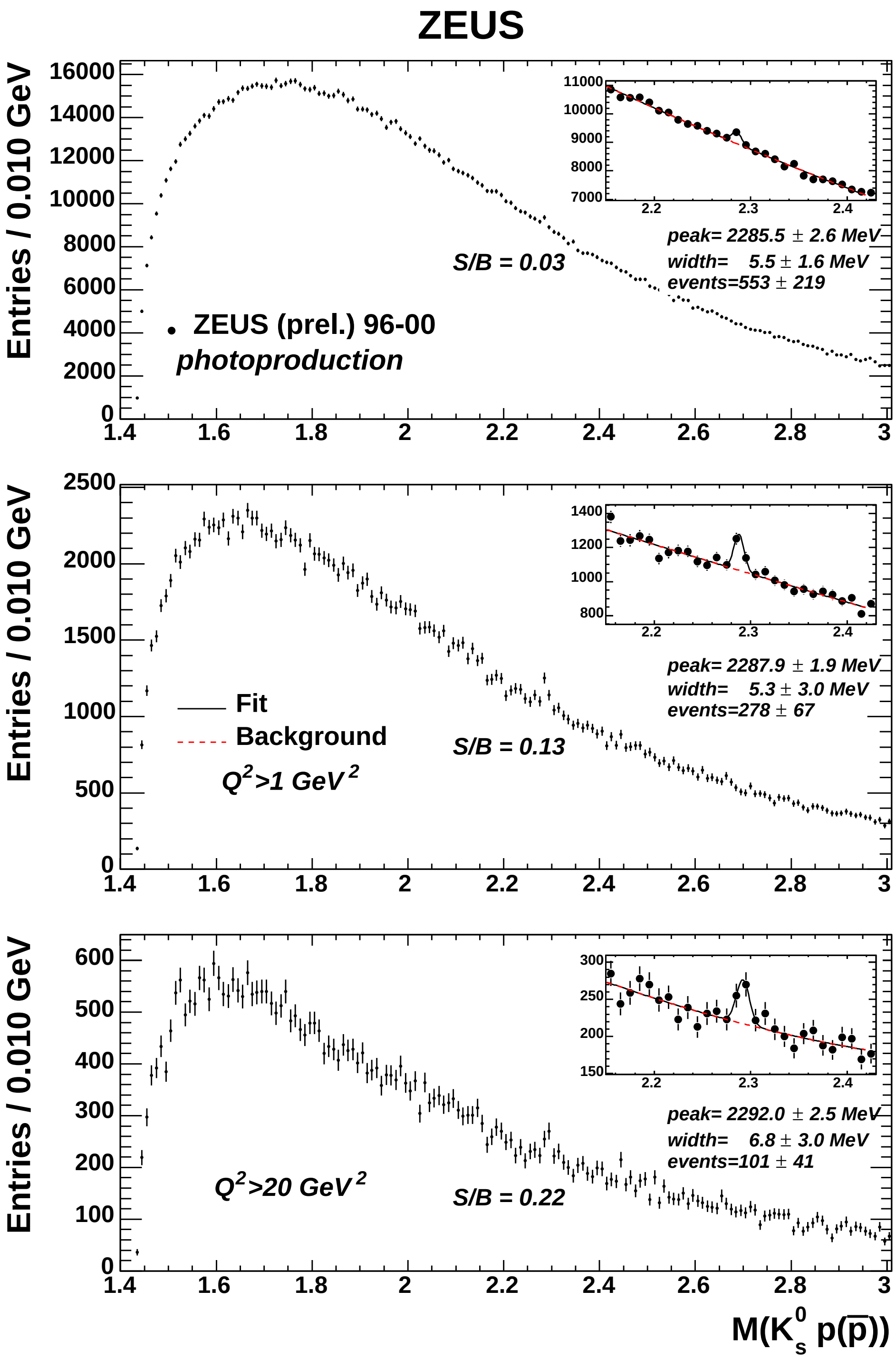

Figure 1: *The $K_S^0\,p$ invariant-mass spectra in PHP and DIS ($Q^2 > 1$ GeV^2 and $Q^2 > 20$ GeV^2). The insets show the invariant-mass distribution near the Λ_c mass region. The solid line shows a fit using a Gaussian plus a second-order polynomial background function using 5 MeV bins. The signal-over-background ratio (S/B) for the Λ_c peak is indicated on each figure.*

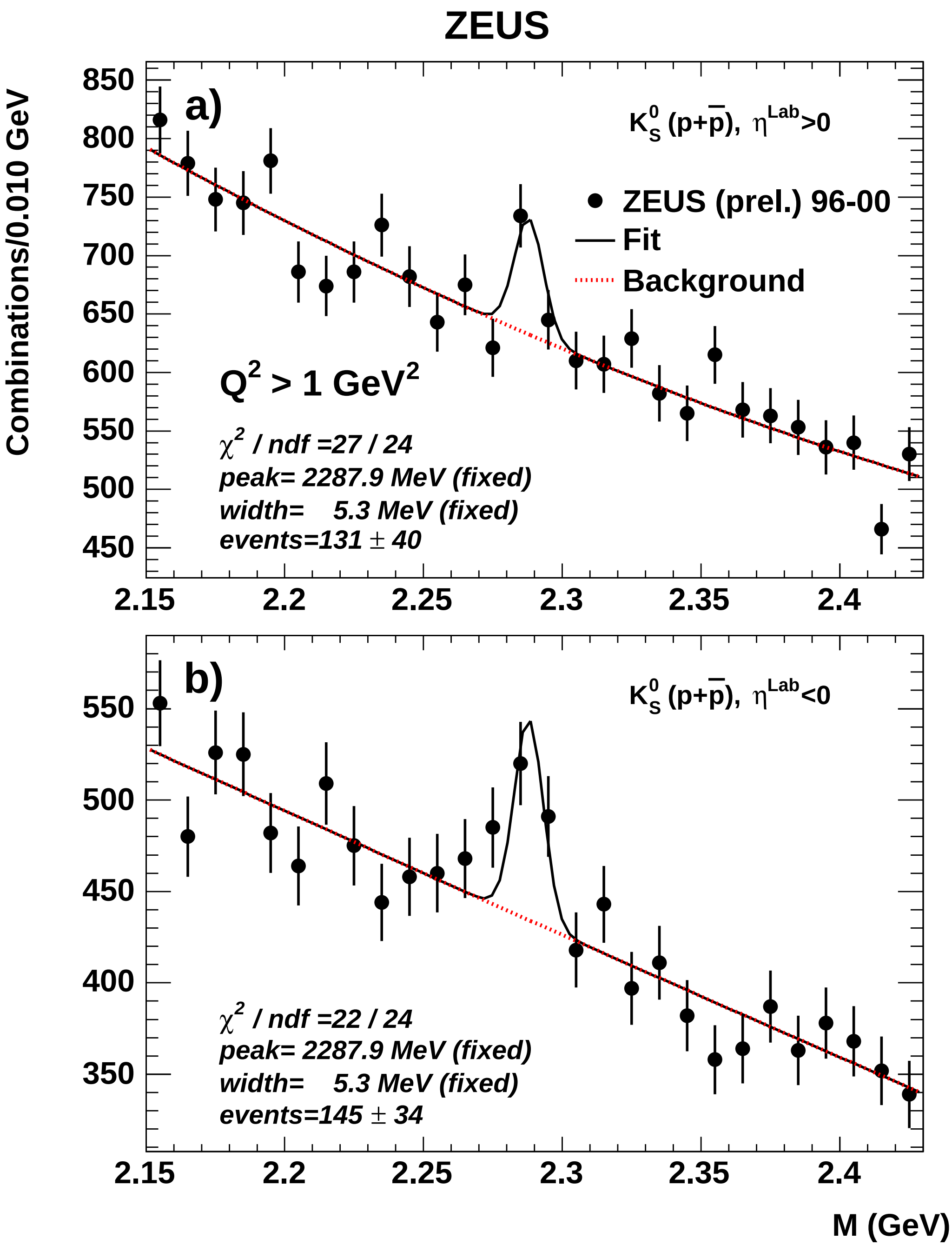

Figure 2: *The $K^0_S p(\bar{p})$ invariant-mass distribution near the Λ_c mass for $\eta > 0$ and $\eta < 0$ regions in DIS for $Q^2 > 1\ GeV^2$. The fit was performed using a Gaussian with a second-order polynomial function. The peak position and the width were fixed from the fit to the sum of these two mass distributions.*

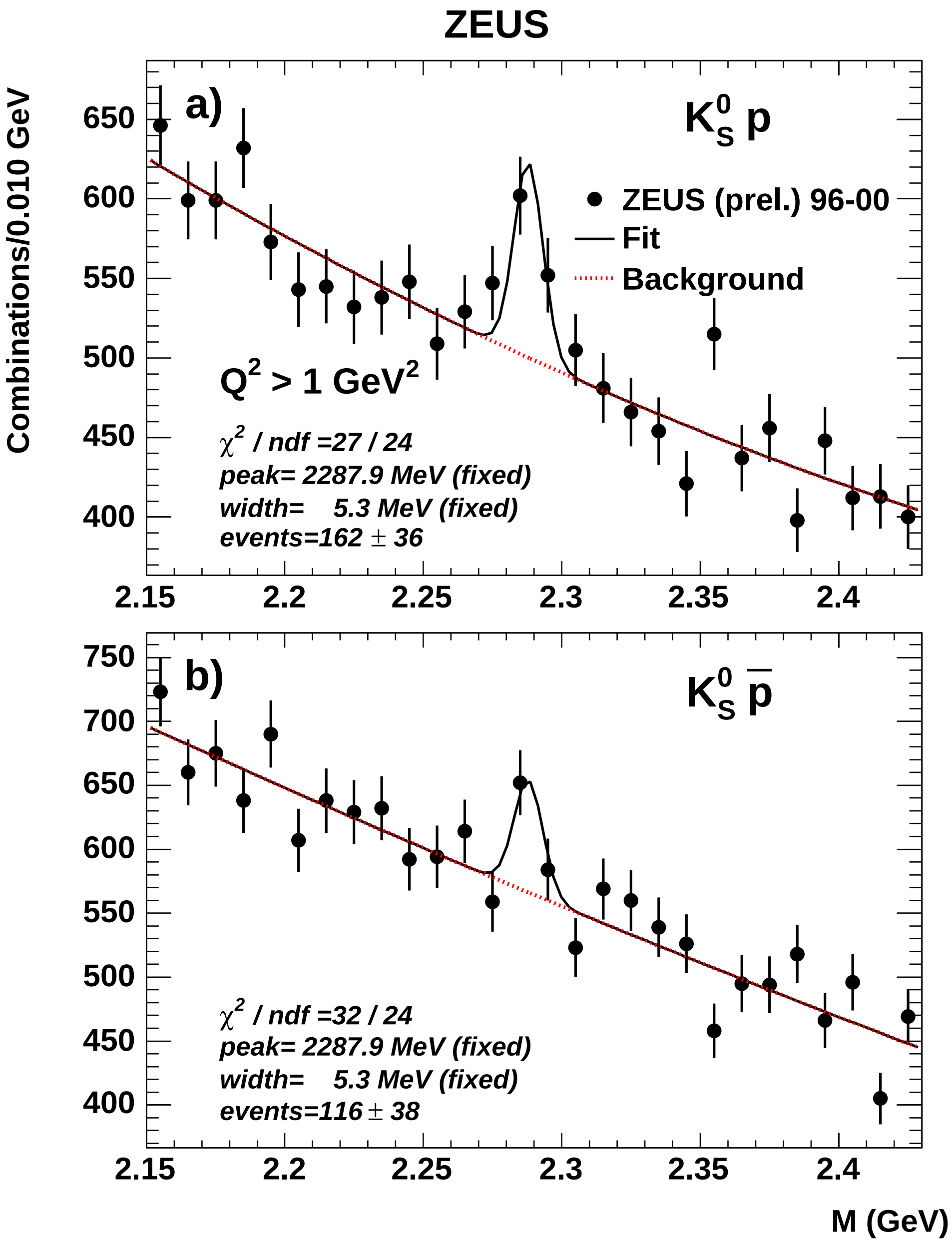

Figure 3: *The invariant-mass distribution near the Λ_c mass for $K^0_S\,p$ and $K^0_S\,\bar{p}$ combinations. The fit was performed using a Gaussian with a second-order polynomial function. The peak position and the width were fixed from the fit to the sum of these two mass distributions.*

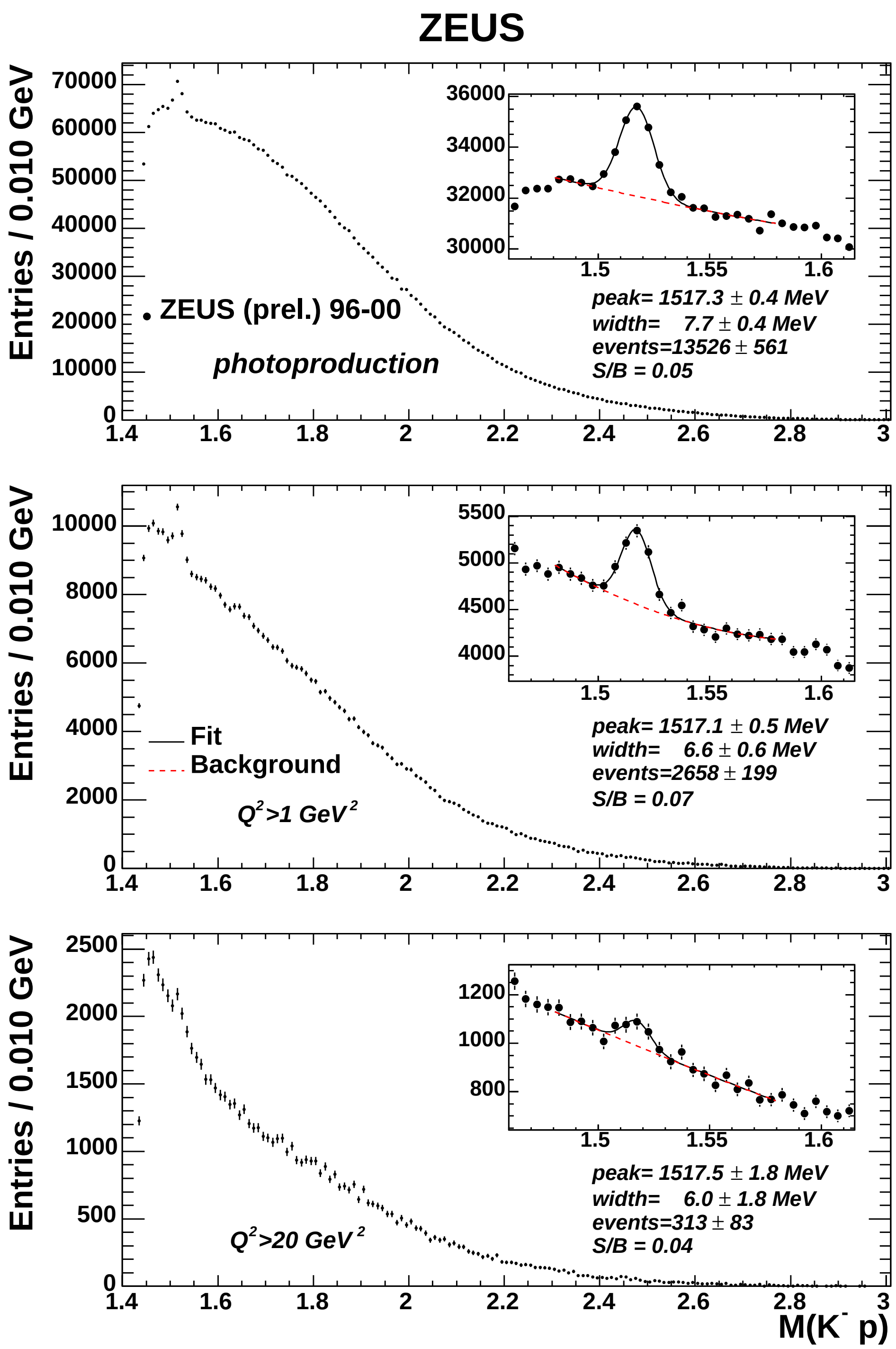

Figure 4: *The K^-p ($K^+\bar{p}$) invariant-mass spectra in PHP and DIS ($Q^2 > 1$ GeV^2 and $Q^2 > 20$ GeV^2). The solid line in the insets shows the result of a fit using a Gaussian plus a second-order polynomial background function. The signal-over-background ratio (S/B) is indicated on each figure.*

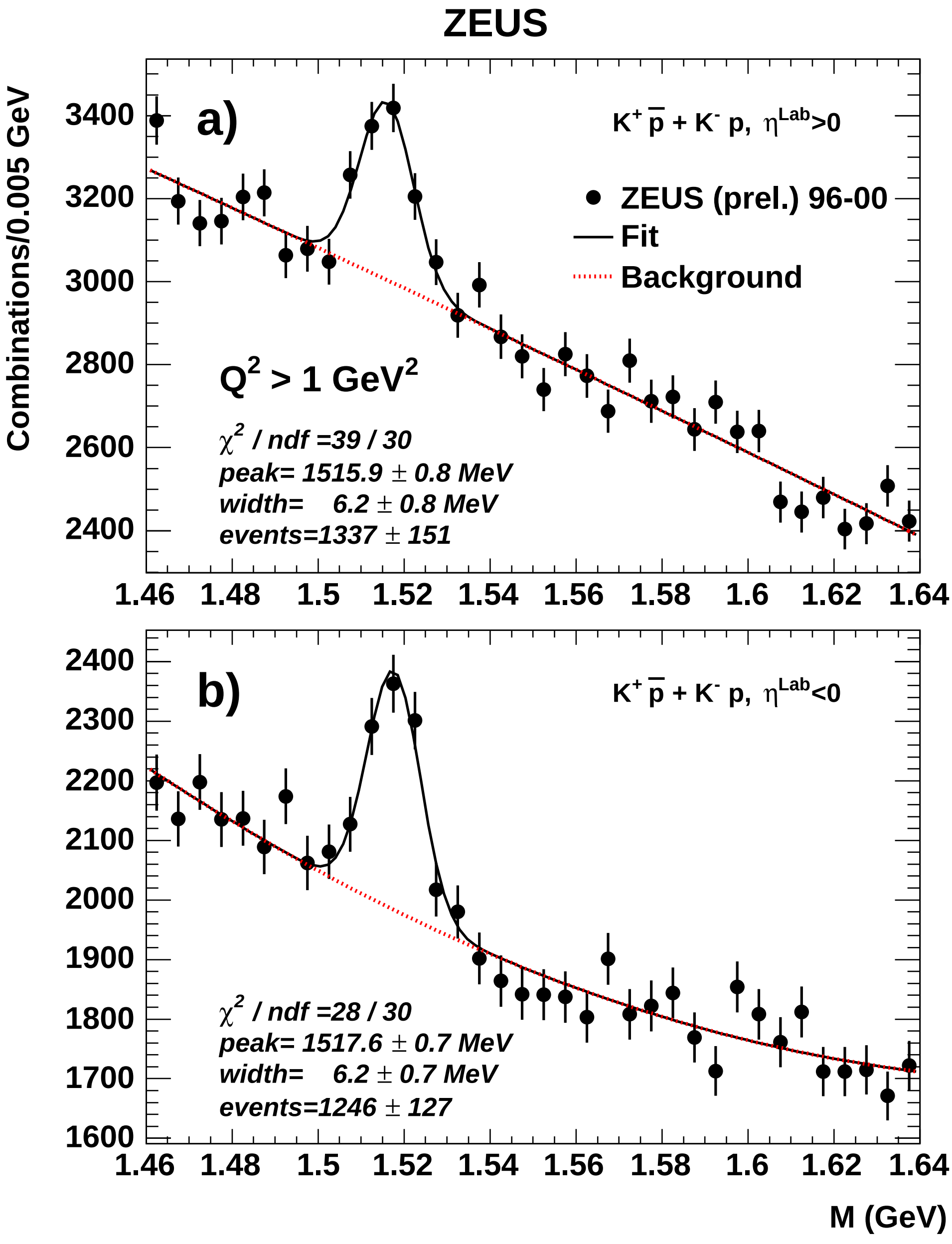

Figure 5: *The $K^-p(K^+\bar{p})$ invariant-mass distribution near the $\Lambda(1520)$ mass in the forward ($\eta > 0$) and in the rear ($\eta < 0$) regions for $Q^2 > 1$ GeV^2. The fit was performed using a Gaussian with a second-order polynomial function.*

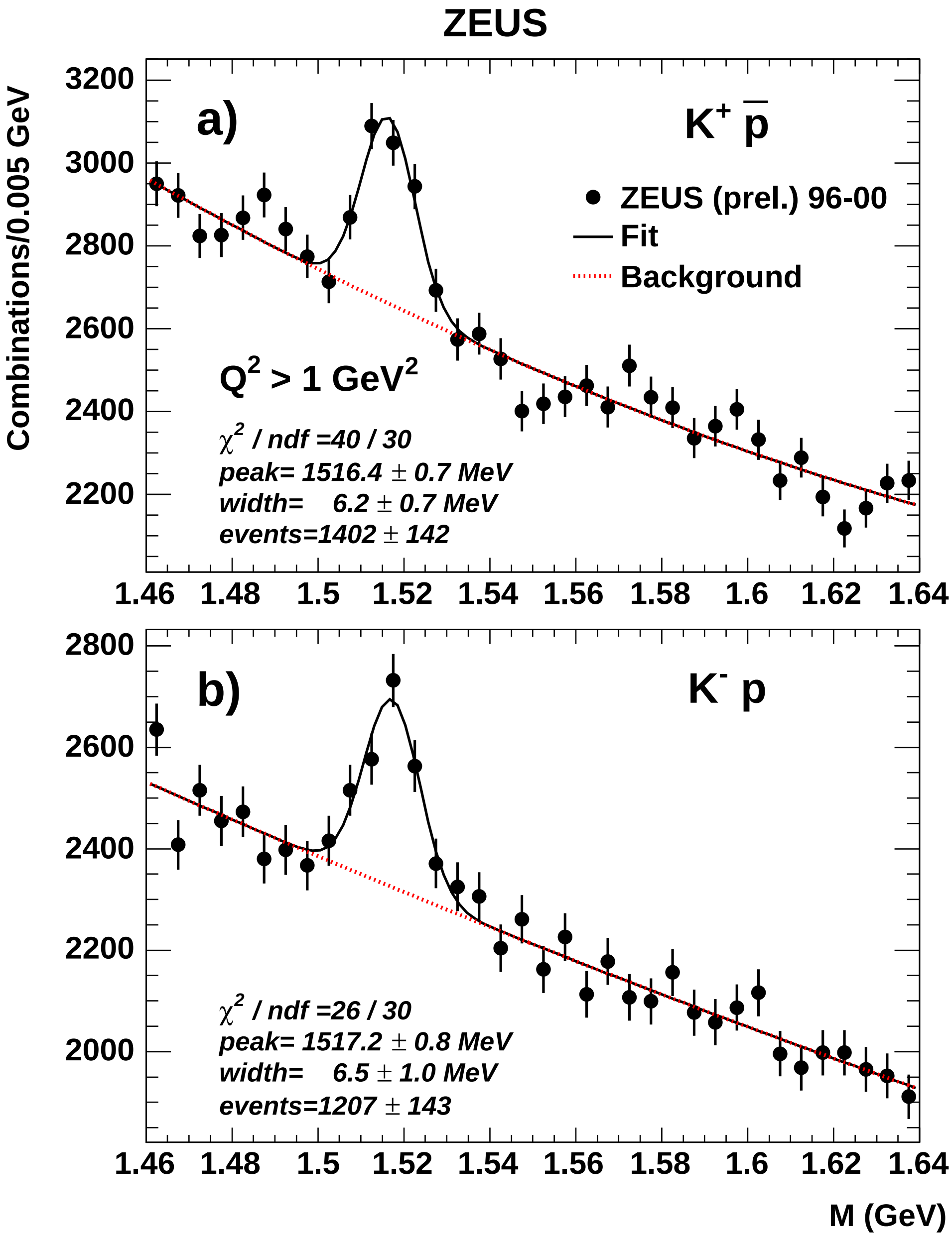

Figure 6: *The invariant-mass distribution near the* $\Lambda(1520)$ *mass region separately for* $K^+\bar{p}$ *and* K^-p *in DIS for* $Q^2 > 1$ GeV^2*. The fit was performed using a Gaussian with a second-order polynomial function.*

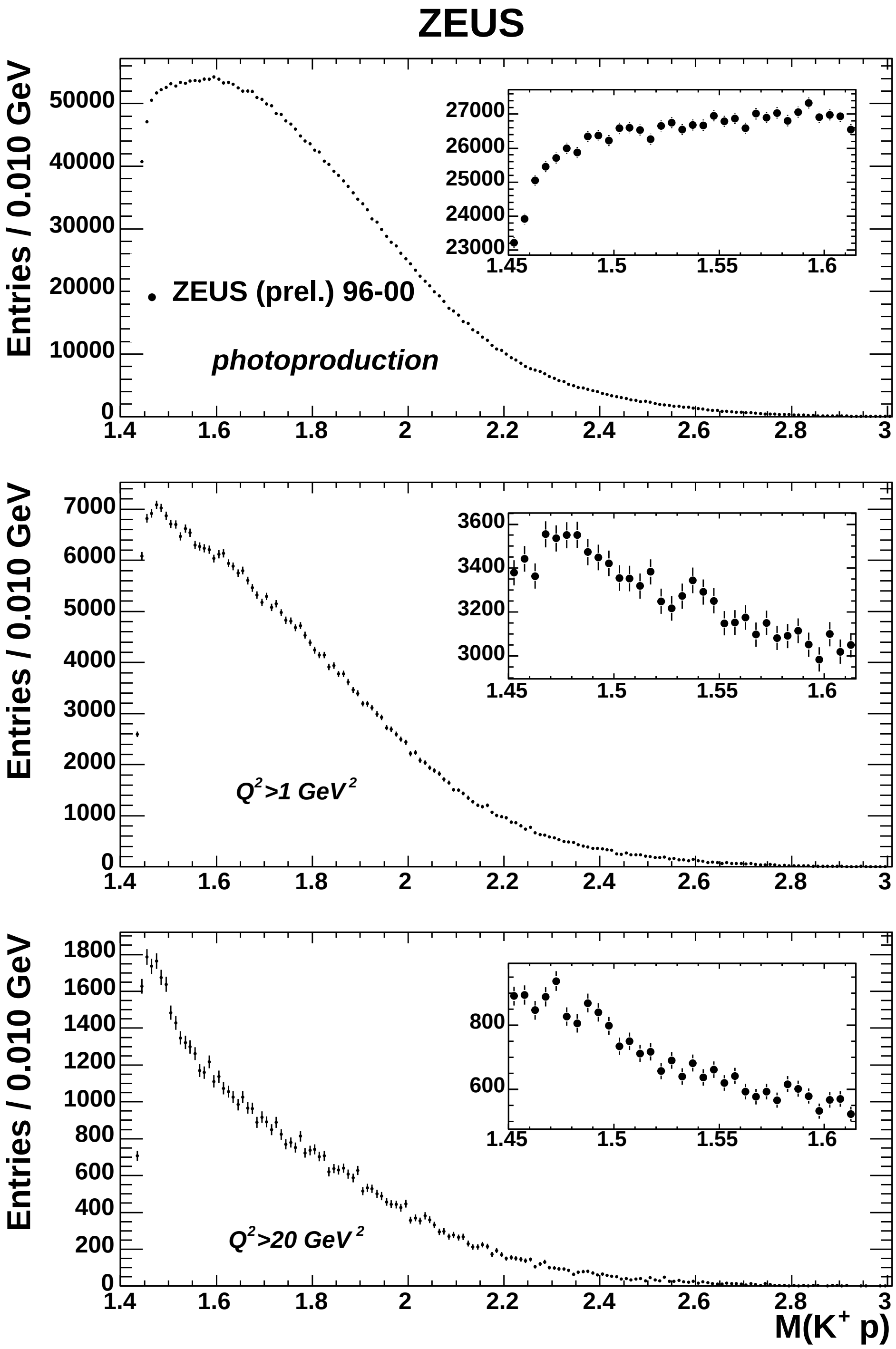

Figure 7: *The K^+p ($K^-\bar{p}$) invariant-mass spectra in PHP and DIS ($Q^2 > 1\ GeV^2$ and $Q^2 > 20\ GeV^2$). The insets show the mass regions with the expected Θ^{++} state. The structure near $1540\ MeV$ for $Q^2 > 1\ GeV^2$ has low statistical significance (about 2σ).*

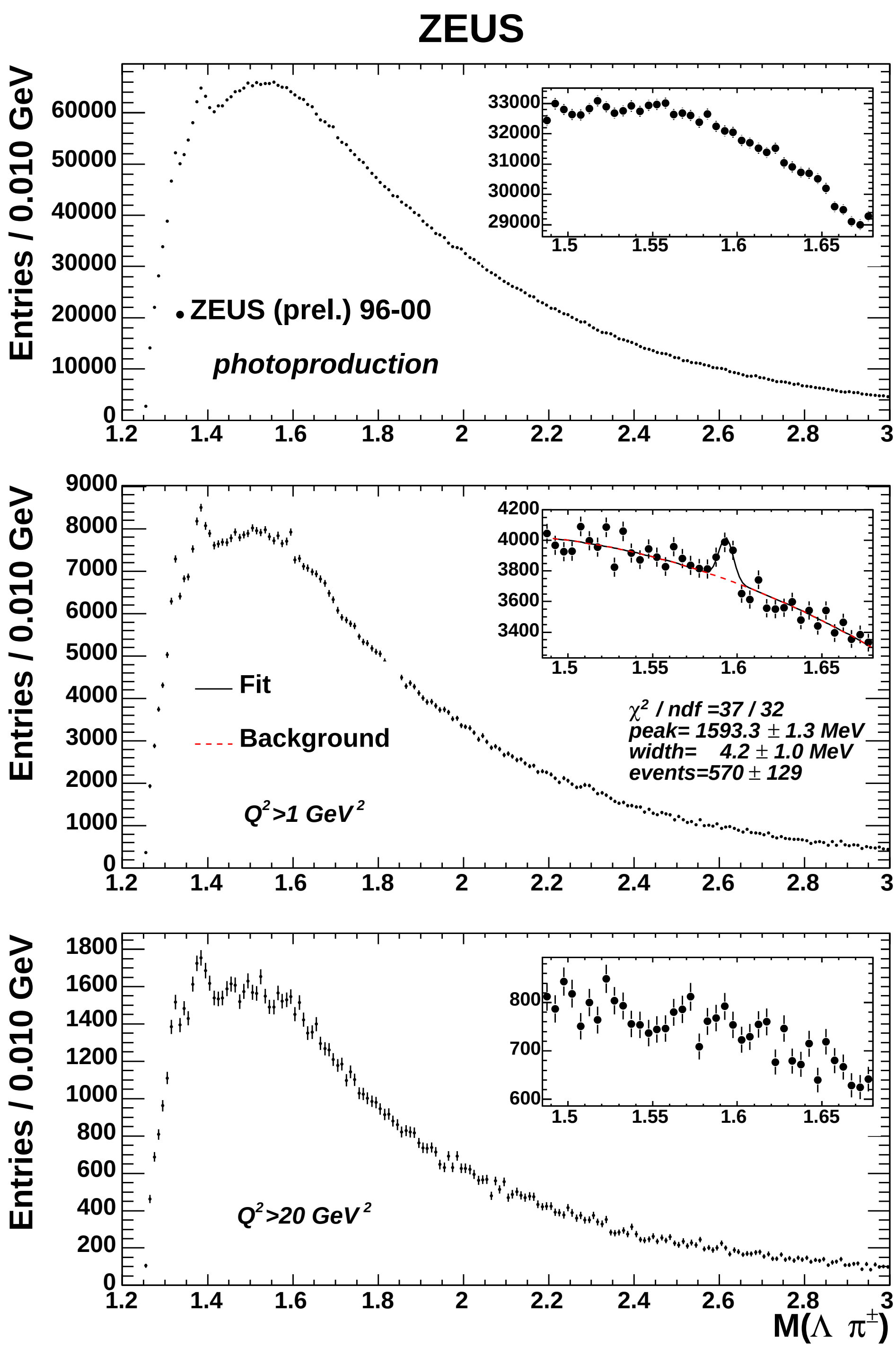

Figure 8: *The $\Lambda\pi$ invariant-mass spectra in PHP and DIS ($Q^2 > 1\,GeV^2$ and $Q^2 > 20\,GeV^2$). The solid line in the inset for $Q^2 > 1\,GeV^2$ shows a fit to a possible resonance near $1600\,MeV$ using a Gaussian with a second-order polynomial background function. The bin width for the insets is $5\,MeV$.*

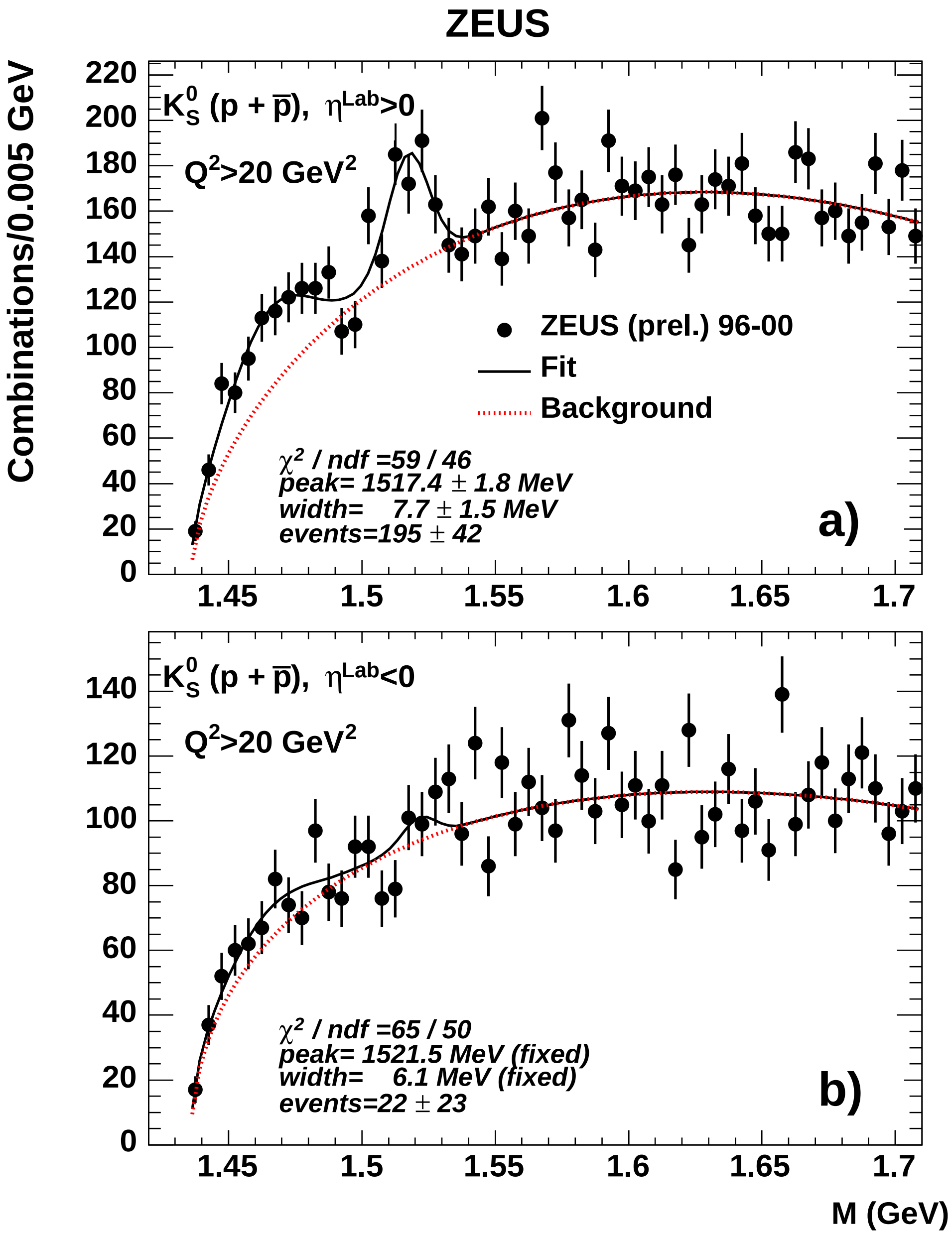

Figure 9: *The $K^0_S\,p\,(\bar{p})$ invariant-mass distribution near the 1520 MeV mass for the forward ($\eta > 0$) and rear ($\eta < 0$) region in DIS for $Q^2 > 20\,GeV^2$. The fit was performed using a double Gaussian with the threshold function: $P_1(M - m_p - m_{K^0_S})^{P_2} \times (1 + P_3(M - m_p - m_{K^0_S}))$, where M is the $K^0_S\,p\,(\bar{p})$ candidate mass, m_p and $m_{K^0_S}$ are the masses of the proton and the K^0_S, respectively, and P_1, P_2 and P_3 are parameters. For the fit in the $\eta < 0$ region, the peak position and the Gaussian width were fixed to the sum of these two distributions.*

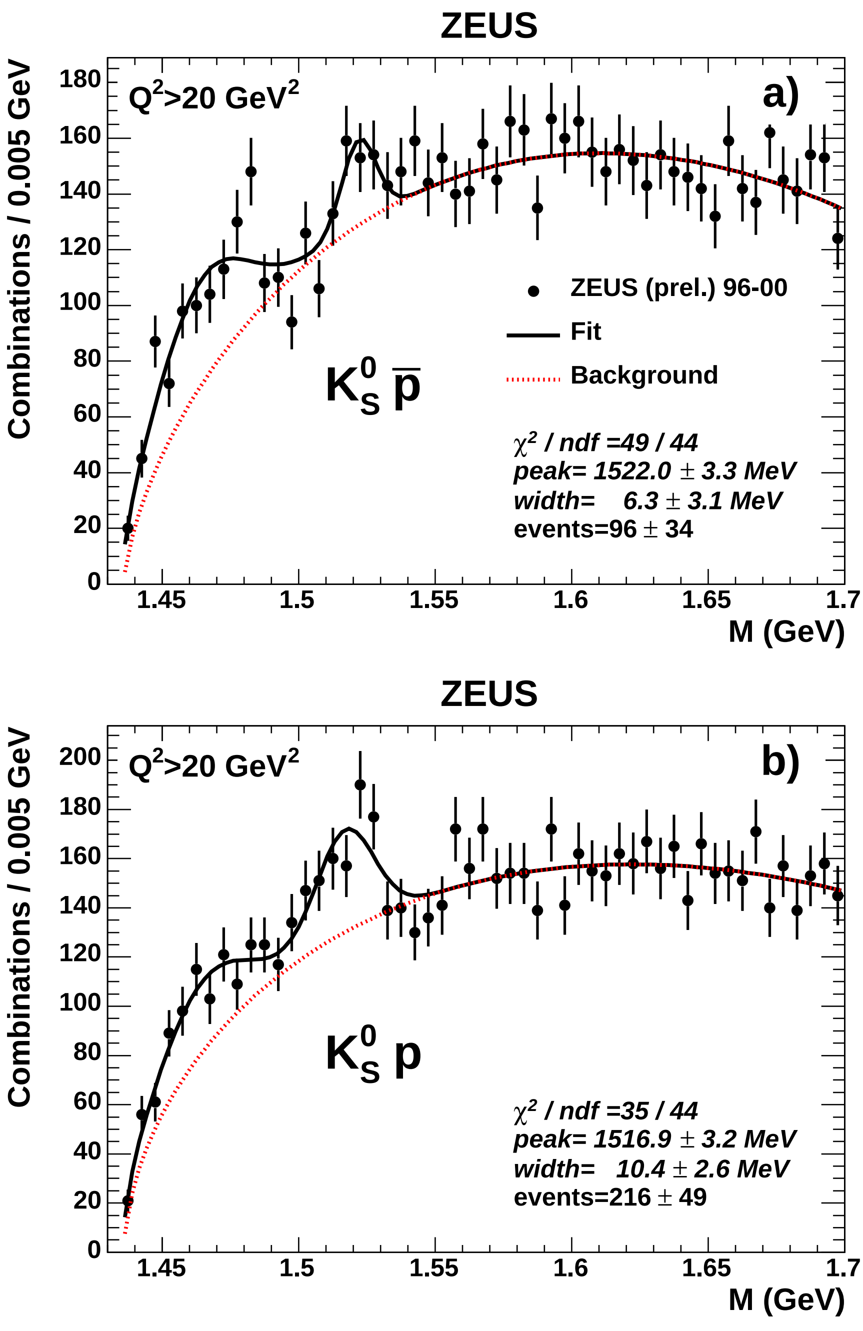

Figure 10: *The invariant-mass distribution near the* 1520 *MeV mass region separately for* $K^0_S\,p$ *and* $K^0_S\,\bar{p}$ *combinations. The fit was performed using a double Gaussian with the threshold function as for Fig. 9. The peak position and the width were fixed to the sum of these two distributions.*

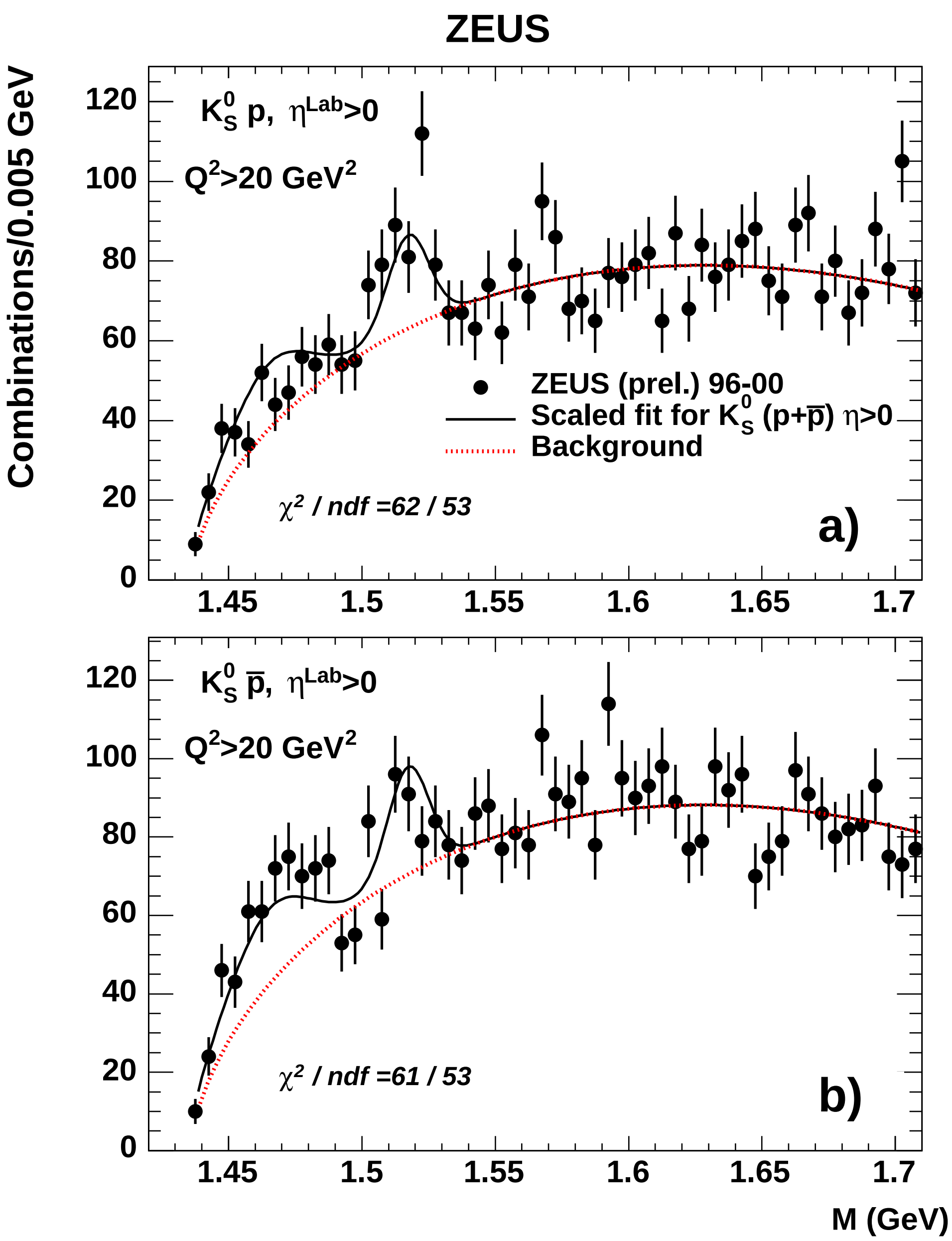

Figure 11: *The invariant-mass distribution separately for the $K^0_S\,p$ and $K^0_S\,\bar{p}$ channels in the forward ($\eta > 0$) region for $Q^2 > 20$ GeV^2. The lines represent fits using a double Gaussian with the threshold function as for Fig. 9. All parameters are fixed from the overall distribution except for one parameter describing the overall normalisation of the entire fitting function.*

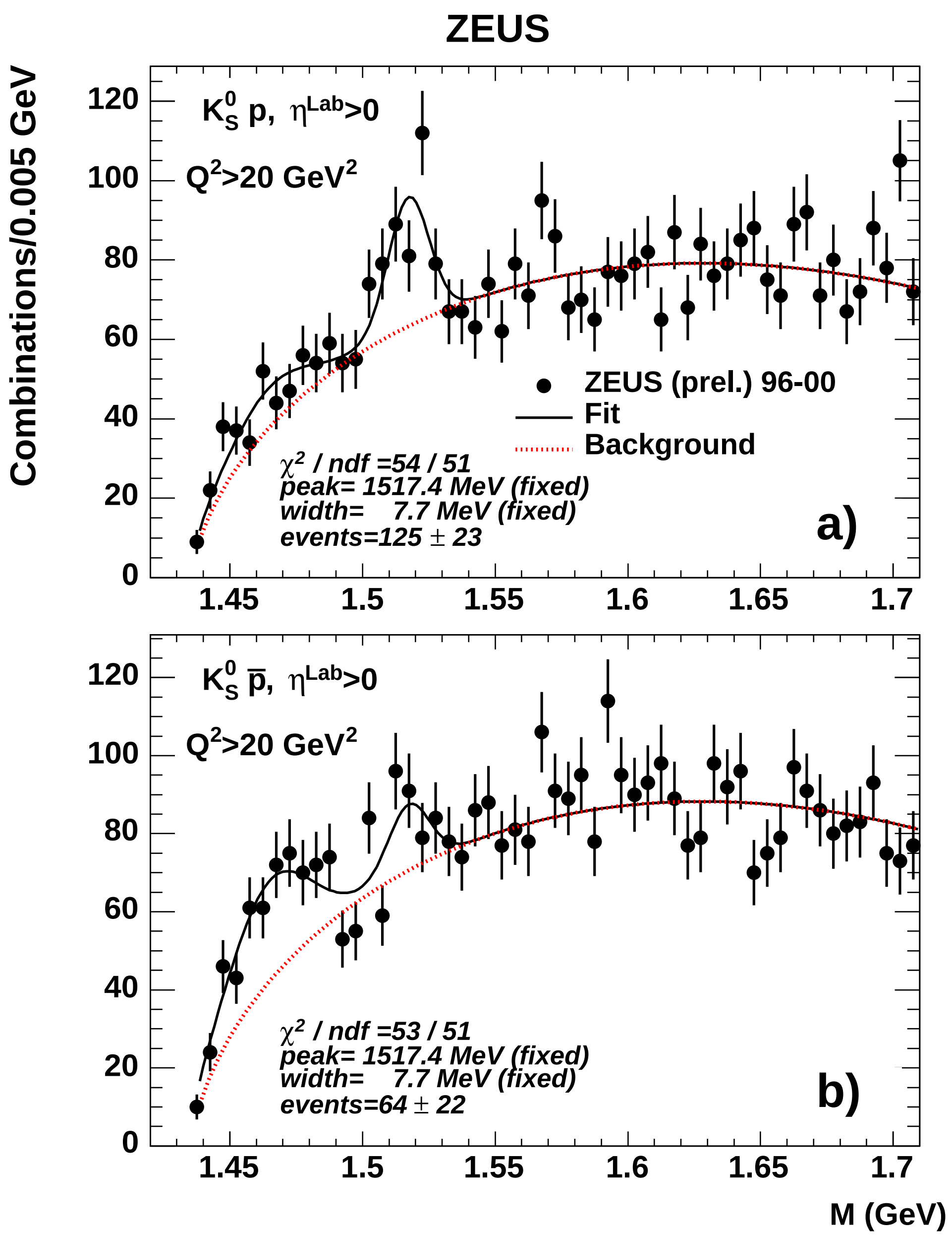

Figure 12: *The invariant-mass distribution separately for the $K^0_S\,p$ and $K^0_S\,\bar{p}$ channels in the forward ($\eta > 0$) region for $Q^2 > 20\ GeV^2$. The lines represent the fits using a double Gaussian with the threshold function as for Fig. 9. Two parameters for the numbers of events in the peaks and one parameter for the background normalisation were not fixed.*